

Sum-of-Norms Periodic Model Predictive Control for Space Rendezvous

Mirko Leomanni, Gianni Bianchini, Andrea Garulli, Renato Quartullo

Abstract—Model Predictive Control is receiving increasing attention in space applications, as a key technology for enhancing autonomy of the flight control system. Sum-of-norms formulations are specifically suited to this context, because they allow to optimize meaningful performance figures and to promote control sparsity. This paper presents a sum-of-norms model predictive control scheme for linear periodically time-varying systems. Closed-loop stability is proven by suitably defining periodic sequences of terminal weights and terminal sets. The proposed solution is applied to a rendezvous case study involving periodic dynamics due to geopotential effects and solar eclipses.

Index Terms—Satellites, Predictive Control for Linear Systems, Time-varying Systems

I. INTRODUCTION

The quest for autonomy is a pervasive aspect of many upcoming space missions. In-orbit operations such as rendezvous, docking and spacecraft formation flying call for complex tasks to be performed autonomously by the onboard flight control system. In this context, a technology which has gained increasing attention in recent years is Model Predictive Control (MPC) [1]. With respect to other control techniques, MPC is able to handle constraints on the state and input signals which are of paramount importance in aerospace applications. MPC schemes have been thoroughly investigated for spacecraft proximity maneuvering, see, e.g., [2], [3], [4], [5]. In these works, a quadratic cost function is employed within the framework of constrained linear-quadratic optimal control theory. However, a quadratic cost function is not always representative of the actual performance requirements put forth by space missions, most prominently fuel optimization. In fact, in many space applications, the mission performance requirements turn out to be correctly described by a sum of vector norms. Besides optimizing fuel consumption, sum-of-norms MPC formulations are known to promote control sparsity, which is instrumental to minimize wear of the propulsion system [6], [7]. However, they typically require a more complex stability analysis, in order to guarantee both recursive feasibility of the MPC policy and the existence of a suitable Lyapunov function [8], [9].

Another specific feature of spacecraft control problems is that they involve periodically time-varying dynamics (see, e.g., [10], [11], [12]). Periodicity may originate from different factors, such as the orbital dynamics of elliptical formations, geopotential effects, eclipses and many others. Linear time-periodic (LTP) systems have been intensively investigated in the literature [13]. Receding-horizon control techniques

for unconstrained LTP systems have been initially studied in [14], [15]. More recently, MPC solutions for constrained LTP systems have been proposed in [16], [17]. These two contributions adopt a standard quadratic cost function, in order to enforce closed-loop asymptotic stability. In the former, recursive feasibility is guaranteed by means of a periodically time-varying ellipsoidal terminal set, which is computed via linear matrix inequalities (LMI). In the latter, a polytopic terminal set is employed, whose computation relies on the theory of periodic controlled invariant sets [18].

This paper presents a sum-of-norms MPC solution for systems with LTP dynamics, which is tailored to space rendezvous control problems. Its main contribution is twofold. On the theoretical side, closed-loop exponential stability of such an MPC scheme is proven. The key feature of the stability proof is the construction of a suitable periodic function, to be used as terminal cost. The proposed terminal cost takes on the form of a weighted 2-norm of the predicted final state, which is defined by a periodic sequence of matrices, obtained from the solution of a periodic Lyapunov equation. This is done via a nontrivial extension of the results in [6] to the LTP case, which allows one to include state constraints and to derive less conservative LMI conditions for the design of the terminal set.

The second contribution is the application of the proposed MPC scheme to a low-thrust rendezvous case study. The considered dynamic model involves periodic effects due to the second zonal harmonic of the geopotential and to solar eclipses. Two different thrusting modes are considered, which correspond to different choices of the input signal norm in both the cost function and the constraints of the MPC problem. Simulation results show the benefits of the new formulation, in terms of convergence speed, sparsity of the thrust command and disturbance rejection. Preliminary work leading to this paper has been presented in [19].

The paper is organized as follows. The baseline sum-of-norms periodic MPC problem is formulated in Section II. Stability results for this problem are presented in Section III, while in Section IV they are extended to the case of polyhedral input norms. The rendezvous case study is described in Section V. The results of the numerical simulations are discussed in Section VI, and Section VII provides some concluding remarks.

Notation and preliminaries

For a real vector $x \in \mathbb{R}^n$, $\|x\|_p$ denotes its p -norm (for brevity, its 2-norm is written as $\|x\|$), while for a matrix $P \in \mathbb{R}^{n \times n}$, $\|P\|$ denotes the induced matrix 2-norm. For a symmetric real matrix P , $\lambda_m(P)$ indicates its minimum

The authors are with the Dipartimento di Ingegneria dell'Informazione e Scienze Matematiche, Università di Siena, Siena, Italy. Email: {leomanni,giannibi,garulli,quartullo}@diism.unisi.it

eigenvalue, while $P > 0$ ($P \geq 0$) denotes (semi)positive definiteness. The p -th row of a matrix M is denoted by $M^{[p]}$. The following definitions are also in order.

Definition 1: For given $N \in \mathbb{N}$, a matrix sequence M_k is termed N -periodic if it satisfies $M_k = M_{k+N} \forall k \in \mathbb{N}$.

Definition 2: An N -periodic matrix sequence X_k is said to be a solution of the N -periodic LMI

$$\mathcal{L}(X_k, X_{k+1}) \leq 0 \quad (1)$$

if (1) holds for all $k \in \mathbb{N}$. Clearly, if matrices X_0, \dots, X_N with $X_N = X_0$ satisfy (1) for $k = 0, \dots, N-1$, then the N -periodic sequence X_k such that $X_k = X_{(k \bmod N)}$ is a solution for all $k \in \mathbb{N}$. The same definition applies to a N -periodic Lyapunov equation of the form $A_k^T X_{k+1} A_k - X_k - Q_k = 0$, where Q_k is N -periodic.

II. PROBLEM FORMULATION

Consider the periodic discrete-time linear system of the form

$$x(k+1) = A_k x(k) + B_k u(k), \quad (2)$$

where $k \in \mathbb{N}$, $x(k) \in \mathbb{R}^n$ is the system state, $u(k) \in \mathbb{R}^m$ is the control input, and system matrices $A_k \in \mathbb{R}^{n \times n}$ and $B_k \in \mathbb{R}^{n \times m}$ are N -periodic for a given period N .

The objective of the control problem considered in this paper is to exponentially stabilize the origin of system (2) via an MPC scheme, in which a sum-of-norms objective function and norm-bounded controls are employed. The 2-norm case is discussed in this section, while polytopic norms are treated in Section IV.

The proposed MPC design is based on the solution, at each time instant $k \in \mathbb{N}$, of the following optimization problem:

$$\begin{aligned} \min_{\hat{\mathcal{U}}_k} & J_k(\hat{\mathcal{U}}_k) \\ \text{s.t.} & \hat{x}_k(0) = x(k) \\ & \hat{x}_k(j+1) = A_{k+j} \hat{x}_k(j) + B_{k+j} \hat{u}_k(j) \\ & \hat{x}_k(j) \in \mathbb{X}_{k+j} \\ & \|\hat{u}_k(j)\| \leq 1 \quad j = 0 \dots H-1 \\ & \hat{x}_k(H)^T S_{k+H} \hat{x}_k(H) \leq 1, \end{aligned} \quad (3)$$

where $\mathbb{X}_k = \mathbb{X}_{k+N}$ is a periodic convex constraint set of the form

$$\mathbb{X}_k = \left\{ x \in \mathbb{R}^n : x^T \Phi_k^l x + F_k^l x + f_k^l \leq 0, \quad l = 1 \dots L \right\} \quad (4)$$

with nonempty interior containing the origin, H is a given time horizon length, $\hat{x}_k(j)$ denotes the predicted state j steps ahead of k , the decision variables are the elements of the control sequence

$$\hat{\mathcal{U}}_k = \{\hat{u}_k(0), \dots, \hat{u}_k(H-1)\}, \quad (5)$$

and the objective function $J(\hat{\mathcal{U}}_k)$ is chosen as

$$J_k(\hat{\mathcal{U}}_k) = \sum_{j=0}^{H-1} \left\{ \|Q \hat{x}_k(j)\| + \|\hat{u}_k(j)\| \right\} + \|W_{k+H} \hat{x}_k(H)\|. \quad (6)$$

In (3),(6), Q is a full-rank matrix, while W_{k+H} and S_{k+H} are full-rank matrices belonging to N -periodic sequences W_k and $S_k = S_k^T$, respectively. As it is well-known, the characterization of the terminal set defined by S_k and of the terminal cost defined by W_k is crucial for stability assessment of the MPC scheme.

Problem (3) is a convex second order cone program (SOCP) which is solved at each discrete-time step k . Then, in the standard receding horizon fashion, the first element of the optimal solution

$$\hat{\mathcal{U}}_k^* = \{\hat{u}_k^*(0), \dots, \hat{u}_k^*(H-1)\} \quad (7)$$

is applied to the system, i.e.,

$$u(k) = \hat{u}_k^*(0). \quad (8)$$

Let $V_k(x(k))$ denote the optimal cost of problem (3), i.e.,

$$V_k(x(k)) = J_k(\hat{\mathcal{U}}_k^*). \quad (9)$$

The domain of the function $V_k(x)$ is the set $\mathcal{F}_k \subseteq \mathbb{R}^n$ of all $x \in \mathbb{R}^n$ such that (3) is feasible for $x(k) = x$. Note that \mathcal{F}_k contains the origin.

Exponential stability of the closed-loop system (2) with the control law (8) can be assessed within the Lyapunov framework of [20], by ensuring that problem (3) is recursively feasible and that its optimal cost $V_k(x(k))$ is strictly decreasing along the closed-loop system trajectories. This can be accomplished by suitably designing the N -periodic matrix sequences S_k and W_k , as detailed in the next section.

III. STABILITY RESULT

Assume that system (2) is stabilizable via N -periodic linear feedback [13], and consider an auxiliary asymptotically stabilizing control law

$$u(k) = -K_k x(k), \quad (10)$$

where the feedback gain $K_k \in \mathbb{R}^{m \times n}$ is N -periodic. Such control law can be computed, for instance, by solving a periodic Riccati equation or an equivalent set of linear matrix inequalities, see, e.g., [13], [16]. The resulting closed-loop system is given by

$$x(k+1) = (A_k - B_k K_k) x(k) = A_k^{cl} x(k), \quad (11)$$

which is clearly N -periodic. The auxiliary control law (10) is instrumental to the design of S_k and W_k . In particular, the following result characterizes a possible choice of S_k ensuring that problem (3) is recursively feasible.

Proposition 1: Let $S_k = S_k^T \in \mathbb{R}^{n \times n}$, $\alpha_k^l \in \mathbb{R}$ be a solution of the periodic LMI set

$$\begin{aligned} (a) & S_k > 0 \\ (b) & (A_k^{cl})^T S_{k+1} A_k^{cl} - S_k < 0 \\ (c) & S_k \geq K_k^T K_k \\ (d) & \alpha_k^l \begin{bmatrix} \Phi_k^l & \frac{1}{2}(F_k^l)^T \\ \frac{1}{2}F_k^l & f_k^l \end{bmatrix} \leq \begin{bmatrix} S_k & 0 \\ 0 & -1 \end{bmatrix} \\ (e) & \alpha_k^l > 0, \quad l = 1, \dots, L. \end{aligned} \quad (12)$$

If problem (3) is feasible at time k_0 , then it is also feasible for all $k > k_0$.

Proof: Let us define the periodically time-varying region

$$\mathcal{C}_k = \{x \in \mathbb{R}^n : x^T K_k^T K_k x \leq 1\}, \quad (13)$$

i.e., the set of states $x(k)$ for which the control law (10) satisfies the constraint $\|u(k)\| \leq 1$. From (12.a) it follows that $x^T S_k x \leq 1$ implies $x^T (A_k^{cl})^T S_{k+1} A_k^{cl} x \leq 1$. Defining the periodically time-varying region

$$\mathcal{X}_k = \{x \in \mathbb{R}^n : x^T S_k x \leq 1\}, \quad (14)$$

we get that $x \in \mathcal{X}_k$ implies $A_k^{cl} x \in \mathcal{X}_{k+1}$. Thus, (i) $x(k) \in \mathcal{X}_k$ implies $x(k+1) \in \mathcal{X}_{k+1}$, i.e., \mathcal{X}_k is a periodic sequence of positively invariant sets under the control law (10).

Moreover, (ii) $\mathcal{X}_k \subseteq \mathcal{C}_k$ by (12.b), and $\mathcal{X}_k \subseteq \mathbb{X}_k$ by (12.c), for all $k \in \mathbb{N}$.

From properties (i) and (ii), it follows that if $x(k_0) \in \mathcal{X}_{k_0}$, then the control law (10) ensures that the constraints $\|u(k)\| \leq 1$ and $x(k) \in \mathbb{X}_k$ are satisfied for all $k \geq k_0$.

The proposition can now be proved by induction on k . By assumption, (3) is feasible at time k_0 . Suppose (3) is feasible at time k and let $\hat{x}_k^*(j)$ be the value of $\hat{x}_k(j)$ at the optimum. Then, $\hat{x}_k^*(H) \in \mathcal{X}_{k+H}$, which implies $\hat{x}_k^*(H) \in \mathcal{C}_{k+H}$ and $x_k^*(H) \in \mathbb{X}_{k+H}$. Hence, the control sequence

$$\bar{u}_{k+1} = \{\hat{u}_k^*(1), \dots, \hat{u}_k^*(H-1), -K_{k+H} \hat{x}_k^*(H)\} \quad (15)$$

is a feasible solution of (3) at time $k+1$. \blacksquare

Remark 1: Note that, under the assumption that \mathbb{X}_k has a nonempty interior containing the origin, a solution of (12) always exists. Moreover, the terminal sets \mathcal{X}_k are ellipsoids in \mathbb{R}^n with nonempty interior containing the origin. Furthermore, $\mathcal{X}_k \subseteq \mathcal{F}_k$.

The following proposition characterizes a possible choice of W_k guaranteeing that the cost decrease condition is met.

Proposition 2: Let $Y_k^T Y_k$ be a solution to the periodic Lyapunov equation

$$(A_k^{cl})^T Y_{k+1}^T Y_{k+1} A_k^{cl} - Y_k^T Y_k + (\|Q\| + \|K_k\|) D_k = 0, \quad (16)$$

where D_k is a given N -periodic positive definite symmetric matrix sequence. Define

$$W_k = \left(\min_{i \in \{0, \dots, N-1\}} \frac{\lambda_m(D_i)}{\|Y_{i+1} A_i^{cl}\| + \|Y_i\|} \right)^{-1} \cdot Y_k. \quad (17)$$

Then,

$$\|W_{k+1} A_k^{cl} x\| - \|W_k x\| \leq -\|Qx\| - \|K_k x\| \quad \forall x \in \mathbb{R}^n. \quad (18)$$

Moreover, the sequence of optimal objectives $V_k(x(k))$ of problem (3) satisfies

$$V_{k+1}(x(k+1)) - V_k(x(k)) \leq -\|Qx(k)\| \quad (19)$$

along the trajectories of system (2) under the MPC control law (8).

Proof: The fact that $Y_k^T Y_k$ solves (16) implies

$$\begin{aligned} x^T A_k^{clT} Y_{k+1}^T Y_{k+1} A_k^{cl} x - x^T Y_k^T Y_k x \\ + x^T (\|Q\| + \|K_k\|) D_k x = 0 \end{aligned} \quad (20)$$

for all $x \in \mathbb{R}^n$, which is equivalent to

$$\|Y_{k+1} A_k^{cl} x\| - \|Y_k x\| = \frac{-x^T (\|Q\| + \|K_k\|) D_k x}{\|Y_{k+1} A_k^{cl} x\| + \|Y_k x\|}. \quad (21)$$

Using a standard upper bound for the expression on the right hand side of (21), one gets

$$\|Y_{k+1} A_k^{cl} x\| - \|Y_k x\| \leq \frac{-\lambda_m(D_k) (\|Q\| + \|K_k\|)}{\|Y_{k+1} A_k^{cl}\| + \|Y_k\|} \|x\|. \quad (22)$$

Taking into account (17), it follows from (22) that

$$\|W_{k+1} A_k^{cl} x\| - \|W_k x\| \leq -(\|Q\| + \|K_k\|) \|x\| \quad (23)$$

which, being $(\|Q\| + \|K_k\|) \|x\| \geq \|Qx\| + \|K_k x\|$, implies (18).

Consider the feasible solution \bar{u}_{k+1} in (15) at time $k+1$. One has that

$$\begin{aligned} J_{k+1}(\bar{u}_{k+1}) - V_k(x(k)) &= -\|Qx(k)\| - \|u_k^*(0)\| \\ &\quad + \|Q\hat{x}_k^*(H)\| + \|K_{k+H} \hat{x}_k^*(H)\| \\ &\quad + \|W_{k+H+1} A_{k+H}^{cl} \hat{x}_k^*(H)\| - \|W_{k+H} \hat{x}_k^*(H)\|. \end{aligned} \quad (24)$$

By combining (24) with (18) evaluated at time $k+H$ with $x = \hat{x}_k^*(H)$, it follows that

$$J_{k+1}(\bar{u}_{k+1}) - V_k(x(k)) \leq -\|Qx(k)\| - \|u_k^*(0)\|. \quad (25)$$

Finally, since \bar{u}_{k+1} is in general suboptimal at time $k+1$, (19) follows from (25). \blacksquare

The following result establishes bounds on the optimal cost $V_k(x(k))$, which are instrumental to prove exponential stability.

Proposition 3: There exist nonnegative constants c_1 and c_2 such that the optimal cost of problem (3) satisfies

$$c_1 \|x\| \leq V_k(x) \leq c_2 \|x\| \quad \forall x \in \mathcal{F}_k, \quad \forall k \in \mathbb{N}. \quad (26)$$

Proof: The lower bound follows immediately from (6),(9) taking $c_1 := \sqrt{\lambda_m(Q^T Q)}$. By virtue of (18) and the dynamic programming principle, it can be shown that

$$V_k(x) \leq \|W_k x\| \quad \forall x \in \mathcal{X}_k \quad (27)$$

(see Proposition 2.35 in [21]). Let $\mathcal{X} = \bigcap_{i=0}^{N-1} \mathcal{X}_i$, and let $\mathcal{B} \subseteq \mathcal{X}$ denote the largest ball centered at the origin and contained in \mathcal{X} , i.e.,

$$\mathcal{B} = \{x \in \mathbb{R}^n : \|x\| \leq \rho^{-1}\}, \quad \rho = \max_{i \in \{0, \dots, N-1\}} \|S_i\|.$$

From (27) it follows that

$$V_k(x) \leq \max_{i=0, \dots, N-1} \|W_i\| \|x\| := b_1 \|x\| \quad \forall x \in \mathcal{B}, \quad \forall k \in \mathbb{N}. \quad (28)$$

Furthermore, given the form of the objective function (6), the linearity of the system (2), and the constraint $\|\hat{u}_k(j)\| \leq 1$ in problem (3), it follows that there exist $b_2 \geq 0$ and $b_3 \geq 0$ such that $V_k(x) \leq b_2 \|x\| + b_3 \quad \forall x \in \mathcal{F}_k, \quad \forall k \in \mathbb{N}$. Hence, being $\rho \|x\| > 1$ for $x \notin \mathcal{B}$,

$$V_k(x) \leq (b_2 + \rho b_3) \|x\| \quad \forall x \in \mathcal{F}_k \setminus \mathcal{B}, \quad \forall k \in \mathbb{N}. \quad (29)$$

From (28) and (29), it turns out that $V_k(x) \leq (b_1 + b_2 + \rho b_3) \|x\| := c_2 \|x\| \quad \forall x \in \mathcal{F}_k, \quad \forall k \in \mathbb{N}$. \blacksquare

Finally, we are able to state the main stability result.

Theorem 1: The MPC scheme (3)-(8) with S_k and W_k chosen as in Propositions 1-2 renders $x = 0$ exponentially stable for system (2).

Proof: Given recursive feasibility established in Proposition 1 and the fact that $V_k(x)$ in (9) is a time-varying Lyapunov function by virtue of (19) and (26), the result follows from Theorem 2.39 in [21]. In particular, (19) implies

$$V_{k+1}(x(k+1)) - V_k(x(k)) \leq -c_1 \|x(k)\|, \quad (30)$$

and, from (26) and (30), $V_{k+1}(x(k+1)) \leq c_3 V_k(x(k))$ with $c_3 = 1 - c_1/c_2 < 1$, from which exponential stability follows. ■

IV. EXTENSION TO POLYTOPIC INPUT NORMS

In this section, we discuss the extension of the results in Section III to the case where the 1-norm of the control input is considered in the cost function and an ∞ -norm input constraint is enforced. This formulation promotes control sparsity among each individual input channel and is also of interest in spacecraft rendezvous applications as detailed in Section V. We consider the same MPC setting as in Section II with the associated optimization problem defined as

$$\begin{aligned} \min_{\hat{U}_k} \quad & J'_k(\hat{U}_k) \\ \text{s.t.} \quad & \hat{x}_k(0) = x(k) \\ & \hat{x}_k(j+1) = A_{k+j} \hat{x}_k(j) + B_{k+j} \hat{u}_k(j) \\ & \hat{x}_k(j) \in \mathbb{X}_{k+j} \\ & \|\hat{u}_k(j)\|_\infty \leq 1 \quad j = 0 \dots H-1 \\ & \hat{x}_k(H)^T S'_{k+H} \hat{x}_k(H) \leq 1, \end{aligned} \quad (31)$$

where the objective function is given by

$$J'_k(\hat{U}_k) = \sum_{j=0}^{H-1} \left\{ \|Q \hat{x}_k(j)\| + \|\hat{u}_k(j)\|_1 \right\} + \|W'_{k+H} \hat{x}_k(H)\|, \quad (32)$$

and the matrix sequences W'_k and S'_k are full-rank and N -periodic. The stability results in Section III can be extended to problem (31)-(32) as stated next.

Proposition 4: Let $S'_k = (S'_k)^T \in \mathbb{R}^{n \times n}$, $\alpha_k^l \in \mathbb{R}$, $\bar{\beta}_k^p \in \mathbb{R}$, $\underline{\beta}_k^p \in \mathbb{R}$ be a solution of the periodic LMI set

$$\begin{aligned} a) \quad & S'_k > 0 \\ & (A_k^{cl})^T S'_{k+1} A_k^{cl} - S'_k < 0 \\ b) \quad & \bar{\beta}_k^p \begin{bmatrix} 0 & \frac{1}{2}(K_k^{[p]})^T \\ \frac{1}{2}K_k^{[p]} & -1 \end{bmatrix} \leq \begin{bmatrix} S'_k & 0 \\ 0 & -1 \end{bmatrix} \\ & \underline{\beta}_k^p \begin{bmatrix} 0 & -\frac{1}{2}(K_k^{[p]})^T \\ -\frac{1}{2}K_k^{[p]} & -1 \end{bmatrix} \leq \begin{bmatrix} S'_k & 0 \\ 0 & -1 \end{bmatrix} \\ & \bar{\beta}_k^p > 0, \quad \underline{\beta}_k^p > 0, \quad p = 1, \dots, m \\ c) \quad & \alpha_k^l \begin{bmatrix} \Phi_k^l & (F_k^l)^T \\ F_k^l & f_k^l \end{bmatrix} \leq \begin{bmatrix} S'_k & 0 \\ 0 & -1 \end{bmatrix} \\ & \alpha_k^l > 0, \quad l = 1, \dots, L. \end{aligned} \quad (33)$$

where K_k is chosen as discussed after (10). Suppose problem (31) is feasible at time k_0 . Then, it is also feasible for all $k > k_0$ along the trajectories of system (2) under the MPC control law (7)-(8) stemming from the solution of (31)-(32).

Proof: Let $\mathcal{X}'_k = \{x \in \mathbb{R}^n : x^T S'_k x \leq 1\}$. Similarly to what observed in Proposition 1, $x(k) \in \mathcal{X}'_k$ implies $x(k+1) \in \mathcal{X}'_{k+1}$ under the control law (10) by (33) (a). Moreover, (33) (b) ensures that $\|K_k x\|_\infty \leq 1$ for all x such that $x^T S'_k x \leq 1$. The result is then proved by induction in the same fashion as Proposition 1. ■

Theorem 2: The MPC design (31)-(32) with S'_k as in Proposition 4 and

$$W'_k = \sqrt{m} W_k, \quad (34)$$

where W_k is given by Proposition 2, renders $x = 0$ exponentially stable for the closed-loop system (2),(8).

Proof: Recall from Proposition 2 that

$$\|W_{k+1} A_k^{cl} x\| - \|W_k x\| \leq -\|Qx\| - \|K_k x\|. \quad (35)$$

By using (34)-(35) and standard norm inequalities, it follows that

$$\begin{aligned} \|W'_{k+1} A_{cl} x\| - \|W'_k x\| & \leq -\sqrt{m}(\|Qx\| + \|K_k x\|) \\ & \leq -\|Qx\| - \|K_k x\|_1. \end{aligned} \quad (36)$$

By adopting the same reasoning as in Proposition 2, it can be concluded that the optimal cost $V'(x(k))$ of (31) satisfies

$$V'_{k+1}(x(k+1)) - V'_k(x(k)) \leq -\|Qx(k)\|. \quad (37)$$

Since recursive feasibility is guaranteed according to Proposition 4, exponential stability of $x = 0$ can be concluded along the same lines as Proposition 3 and Theorem 1. ■

V. APPLICATION TO SPACE RENDEZVOUS

In this section, the proposed MPC methodology is applied to a space rendezvous problem. The classical scenario in which the spacecraft must reach a predefined rendezvous point, along the target orbit, is considered. In this context, system (2) describes the linearized relative motion dynamics and the control objective consists of steering the relative trajectory to the equilibrium point $x = 0$, while achieving a trade-off between fuel consumption and state regulation performance. Furthermore, limitations on the maximum thrust delivered by the propulsion system must be taken into account. The following maneuvering modes are considered for the spacecraft, according to standard design rules.

(A) *Thrust vectoring:* maneuvering is achieved by firing a single thruster and steering the thrust vector via attitude control. In this approach, constraints on the maximum deliverable thrust can be expressed as $\|u(k)\| \leq 1$. The thruster fuel consumption is proportional to $\sum_k \|u(k)\|$.

(B) *Thrust allocation:* maneuvering is achieved by firing a set of orthogonal thrusters producing thrust along the basis vectors of a local orbital frame. In this setting, the control bounds can be modeled as $\|u(k)\|_\infty \leq 1$. The fuel consumption of the propulsion system is proportional to $\sum_k \|u(k)\|_1$. Clearly, the control mode (A) can be tackled by using the formulation in Section II, while the formulation in Section

IV fits case (B). In the following, additional details about the relative motion dynamics are provided. In particular, it will be shown that the considered LTP framework allows one to effectively describe Earth's oblateness and solar eclipse effects.

A. Relative motion dynamics

For the purpose of control design, a linearized dynamic model based on the relative motion parameterization introduced in [22] is adopted. Such a parameterization provides a nonsingular relative motion description and retains a simple relationship with local orbital coordinates. The main steps involved in the derivation of the linearized model are discussed below. The rendezvous point is modeled as an orbiting point-mass particle, which is denoted as *satellite 1*. The controlled spacecraft is denoted as *satellite 2*. Let the *relative line of nodes* be defined as the intersection of the orbital planes of the two satellites. The angle between these planes is the relative inclination γ . Moreover, let λ_j and θ_j be the angles formed respectively by the periapsis of orbit j and the position vector of satellite j with respect to the relative line of nodes. The relative motion between the two satellites is parameterized by the state vector $x = [x_1, \dots, x_6]^T$, defined by

$$\begin{aligned} x_1 &= \theta_2 - \theta_1 \\ x_2 &= (n_2 - n_1)/n_1 \\ x_3 &= e_2 \cos(\theta_2 - \lambda_2) - e_1 \cos(\theta_2 - \lambda_1) \\ x_4 &= e_2 \sin(\theta_2 - \lambda_2) - e_1 \sin(\theta_2 - \lambda_1) \\ x_5 &= \tan(\gamma/2) \cos \theta_2 \\ x_6 &= \tan(\gamma/2) \sin \theta_2, \end{aligned} \quad (38)$$

where n_j , e_j are the mean motion and the eccentricity of orbit j , respectively. In terms of the parameters (38), the rendezvous condition is $x = 0$. We restrict our attention to satellites in near-circular orbits ($e_1 \approx 0$). The separation between satellite 1 and satellite 2 is assumed to be small compared to the orbit radius. The Earth is modeled as an oblate spheroid. Within this setting, the linearization of the dynamics of the state vector (38) about $x = 0$ and $u = 0$ gives the continuous-time dynamic model

$$\dot{x} = A(t)x + Bu, \quad (39)$$

where u is the control acceleration delivered by satellite 2, expressed in its own local orbital frame. The local orbital frame adopted in this paper is the so-called Radial-Transverse-Normal frame, see, e.g., [23]. The matrix $A(t)$ in (39) turns out to be structured as $A(t) = A_{Kep} + A_{J_2}(t)$, where A_{Kep} models the contribution of spherical gravity, and $A_{J_2}(t)$ describes the secular effects of the zonal harmonic J_2 of the geopotential (i.e., of Earth's oblateness) on the relative orbit configuration. The matrix A_{Kep} reads

$$A_{Kep} = n_1 \begin{bmatrix} 0 & 1 & 2 & 0 & 0 & 0 \\ 0 & 0 & 0 & 0 & 0 & 0 \\ 0 & 0 & 0 & -1 & 0 & 0 \\ 0 & 0 & 1 & 0 & 0 & 0 \\ 0 & 0 & 0 & 0 & 0 & -1 \\ 0 & 0 & 0 & 0 & 1 & 0 \end{bmatrix}.$$

The matrix $A_{J_2}(t)$ is given by

$$A_{J_2}(t) = \kappa \begin{bmatrix} 0 & 14c/3 & 2c & 0 & a_{15}(t) & a_{16}(t) \\ 0 & 0 & 0 & 0 & 0 & 0 \\ 0 & 0 & 0 & -c & 0 & 0 \\ 0 & 0 & c & 0 & 0 & 0 \\ 0 & a_{52}(t) & 0 & 0 & a_{55}(t) & a_{56}(t) \\ 0 & a_{62}(t) & 0 & 0 & a_{65}(t) & a_{66}(t) \end{bmatrix},$$

where $c = 3 \cos^2 i_1 - 1$, i_1 is the inclination of satellite 1, $\kappa = 3 J_2 R_e^2 n_1^{7/3} / (4 \mu^{2/3})$ is a constant proportional to J_2 , R_E is the Earth radius, μ is the gravitational parameter, and

$$\begin{aligned} a_{15}(t) &= -14 \sin(2i_1) \cos \varphi(t) \\ a_{16}(t) &= -14 \sin(2i_1) \sin \varphi(t) \\ a_{52}(t) &= -7 \sin(2i_1) \sin \varphi(t)/6 \\ a_{55}(t) &= \sin^2 i_1 \sin(2\varphi(t)) \\ a_{56}(t) &= 2 \sin^2 i_1 [5 - \cos^2 \varphi(t)] - 6 \\ a_{62}(t) &= 7 \sin(2i_1) \cos \varphi(t)/6 \\ a_{65}(t) &= 2 \sin^2 i_1 [\sin^2 \varphi(t) - 5] + 6 \\ a_{66}(t) &= -\sin^2 i_1 \sin(2\varphi(t)). \end{aligned}$$

The angle $\varphi(t)$ in the above equations is the argument of latitude of satellite 1. It is T -periodic in t , where $T = 2\pi/[n_1 + 2\kappa(4 \cos^2 i_1 - 1)]$ is the nodal period of satellite 1. Hence, matrix $A_{J_2}(t)$ is T -periodic. The time-invariant input matrix B in (39) is given by

$$B = \frac{1}{(\mu n_1)^{1/3}} \begin{bmatrix} 0 & 0 & 0 \\ 0 & -3 & 0 \\ 0 & 2 & 0 \\ 1 & 0 & 0 \\ 0 & 0 & 1/2 \\ 0 & 0 & 0 \end{bmatrix}.$$

In order to apply the proposed MPC techniques, system (39) is ZOH-discretized with a sampling interval t_s such that $N = T/t_s \in \mathbb{N}$, thus yielding a periodic discrete-time model of the form (2). Moreover, the dimensional unit of the state vector $x(k)$ of system (2) is normalized by the constant factor m_2/F_{max} , where F_{max} is the maximum deliverable thrust and m_2 is the mass of satellite 2. In this setting, the input vector $u(k)$ is related to the actual thrust $F(k)$ by the identity $u(k) = F(k)/F_{max}$. Hence, according to the chosen thrusting mode, thrust constraints can be expressed as (A) $\|u(k)\| \leq 1$ with $F_{max} = \max_u \|u\|$ and (B) $\|u\|_\infty \leq 1$ with $F_{max} = \max_u \|u\|_\infty$, which are consistent with the MPC problem formulations (3) and (31), respectively.

B. Eclipse effects

Besides capturing the J_2 contribution, the considered LTP framework can be used to account for spacecraft power limitations occurring periodically. In particular, in low-thrust scenarios, on-board power is typically not sufficient to operate the thruster when the spacecraft is shadowed from the sun, i.e., during solar eclipses. Eclipses occur whenever the angle θ_{ES} between the Earth and the Sun, seen from the spacecraft, is smaller than the apparent angular size θ_E of the Earth radius plus the apparent angular size θ_S of the Sun

radius. Therefore, the illumination condition can be formalized as (I) $\theta_{ES} > \theta_E + \theta_S$ [24]. A more restrictive condition can be constructed as (I') $\theta_{ES} > \theta_E + \theta_S + d$, where the constant $d > 0$ is an assignable parameter. Given the small inter-satellite separation, one can choose d so as to ensure that if (I') holds for satellite 1, then (I) holds for satellite 2. Since the occurrence of eclipses has approximately the same period T of the satellite 1 orbital dynamics, which are autonomous, (I') can be treated as a time-periodic condition. The error resulting from this approximation can be absorbed in d . Therefore, one can estimate all time intervals in which the controlled spacecraft (satellite 2) is illuminated, within the rendezvous time scale, by just propagating the rendezvous point (satellite 1) motion over a single orbital period. Note that this can be done offline.

According to the above discussion, a conservative estimate of satellite 2 shadow phases can be obtained by evaluating the set of time instants \mathcal{E} in which $\theta_{ES} \leq \theta_E + \theta_S + d$ is satisfied along the trajectory of satellite 1, on the time interval $[0, T]$. Then, thrust limitations due to eclipsing can be modeled by setting the control input matrix to zero whenever $t \pmod{T} \in \mathcal{E}$. For the discrete-time model (2), this amounts to enforcing

$$B_k = 0 \quad \forall k : kt_s \pmod{Nt_s} \in \mathcal{E}. \quad (40)$$

The constraint (40) clearly preserves the periodicity condition $B_{k+N} = B_k$, and provides a convenient way to include eclipse effects in the LTP description (2).

VI. SIMULATION CASE STUDY

In this section, the performance of the proposed MPC design is evaluated through numerical simulations. The considered simulation setting is as follows. The rendezvous point lies on a circular orbit with a semi-major axis equal to 7387.1 km and an inclination of 81 deg. At the beginning of the rendezvous process, the spacecraft is located 1 km below the rendezvous point, out-of-phase by -0.124 deg. The initial inclination difference between the two orbital planes amounts to 0.002 deg. These parameters correspond to an initial displacement of approximately 16 km, and are consistent with the specifications of a mid-range rendezvous maneuver in Low-Earth-Orbit [25]. The characteristics of the spacecraft are representative of a modern 100 kg class minisatellite equipped with Electric Propulsion (EP). The maximum deliverable thrust of the EP unit is set to $F_{max} = 15$ mN, according to the specifications of existing miniaturized Hall effect thrusters, see, e.g., [26] and the μ HETSAT mission [27], one of the first applications of EP on board a multi-purpose microsatellite platform.

The rendezvous maneuver is simulated on a realistic non-linear truth model accounting for all the significant orbital perturbations, i.e., Earth's Gravity, Atmospheric Drag, Lunar Third Body, and Solar Pressure. The sampling interval for the discretization of model (39) is taken as $t_s = T/32$ (corresponding to about 3 minutes). The resulting LTP system (2),(40) satisfies the standard controllability conditions [13]. The prediction horizon of the MPC controller is set to $H = 48$. Such a long horizon is adopted to effectively deal with the limited control authority provided by the EP system. A trial-and-error procedure has been adopted to tune the weighting

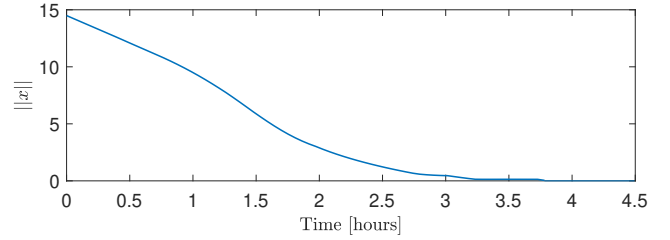


Fig. 1. Thrust vectoring mode: Evolution of the state vector 2-norm.

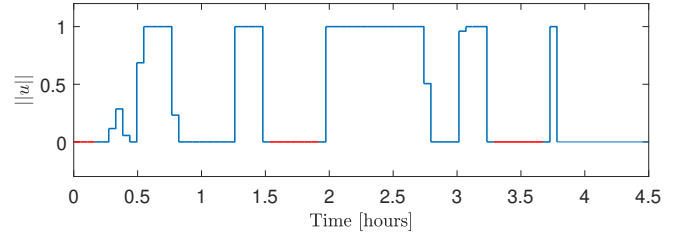


Fig. 2. Thrust vectoring mode: Evolution of the control input vector 2-norm (eclipse phases are highlighted in red).

matrix Q , resulting in $Q = \text{diag}\{5, 2.5, 0.05, 0.05, 0.5, 0.5\}$. The gain matrix K_k in (10) is set as the solution of the standard periodic LQR problem [13] with weight matrices $Q_k^{LQR} = Q^T Q$ and $R_k^{LQR} = I$. The matrix S_{k+H} in (3) is chosen as in Proposition 1. The terminal weight W_{k+H} in (3) is set as in Proposition 2, where for simplicity the matrix D_k is taken as the identity matrix for all k . Note that the above computations are performed offline. The LMIs and the MPC problems are solved by using the package CVX [28] and the commercial solver Gurobi [29].

The *thrust vectoring* control mode is demonstrated by applying the MPC design (3). The evolution of the state vector 2-norm resulting from the rendezvous simulation is depicted in Fig. 1. We observe that in this case the state converges to zero in finite time. Although there is no theoretical guarantee for this behavior, it is interesting to recall that this is the same behavior that was observed in [6] for the LTI case. The control input vector 2-norm is reported in Fig. 2. As expected, the input constraint $\|u(k)\| \leq 1$ is always satisfied, and the command is idle during eclipse phases (highlighted in red). The feedback policy displays a sparse control activation pattern, which is a desirable feature in order to limit the EP system wear. The target is reached in 3.8 h, incurring a fuel cost of $\sum_k \|u(k)\| = 28.8$, which corresponds to a propellant consumption of 7.2 g. This is a relatively modest figure considering the amount of propellant that can be embarked on a microsatellite. In order to illustrate the effect of state constraints, the simulation has been repeated by enforcing a lower bound on the radial separation between the spacecraft and the rendezvous point in the MPC problem formulation. A linearization of such constraint has the form (4) where $L = 1$, $F_k^1 = [0 \ 2/3 \ 1 \ 0 \ 0 \ 0]$, $\Phi_k^1 = 0$ and $f_k^1 < 0$. In this case study, f_k^1 is set to -1.15 . For a detailed description of how constraints on the relative position can be expressed in terms of the parameters (38), see [30]. The resulting in-plane trajectory is compared with the unconstrained one in Fig. 3.

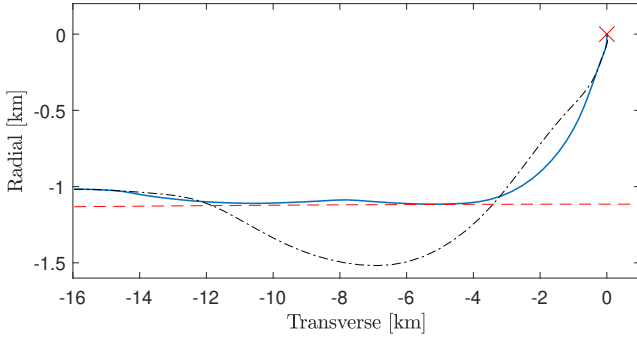


Fig. 3. Thrust vectoring mode: radial and transverse error trajectories in the constrained (solid blue line) and in the unconstrained (black dash-dotted line) case. The constraint (red dashed line) is a lower bound on the radial error.

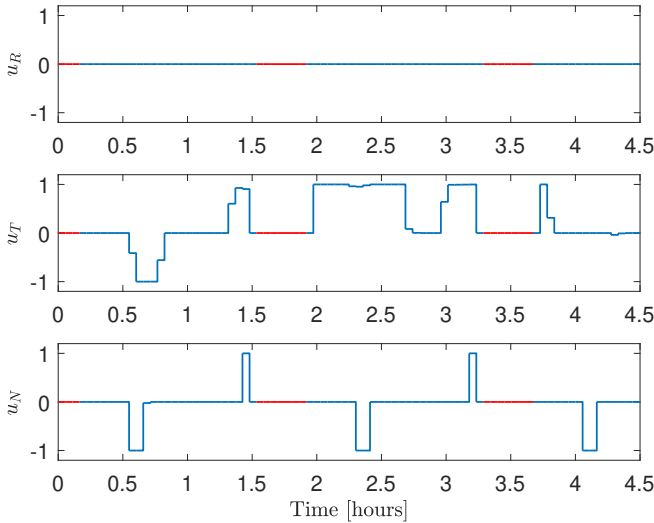


Fig. 4. Thrust allocation mode: Evolution of the Radial, Transverse and Normal components of the control input vector (eclipse phases are highlighted in red).

As expected, the required bound is satisfied when included in the formulation.

The *thrust allocation* control mode is demonstrated by exploiting the results in Section IV. The resulting state vector 2-norm profile is not reported as it matches closely that in Fig. 1. The evolution of the radial, transverse and normal components of the control input vector are reported in Fig. 4. It can be seen that the controller achieves control sparsity on each input channel. Moreover, the input constraint $\|u(k)\|_\infty \leq 1$ is always satisfied. The maneuver completion time is 4.4 h and the fuel cost is $\sum_k \|u(k)\|_1 = 33.9$, which corresponds to a propellant consumption of 8.4 g. In both control modes, the computing time for the solution of a single MPC problem instance is in the order of 1 s (on a standard laptop), i.e., a negligible fraction of the sampling time. A qualitative assessment of the robustness of the MPC design (3) with respect

TABLE I
MEASUREMENT NOISE CHARACTERISTICS

Type	GPS (absolute states)	DGPS (relative states)
Position std	10 m	1 m
Velocity std	0.2 m/s	0.02 m/s

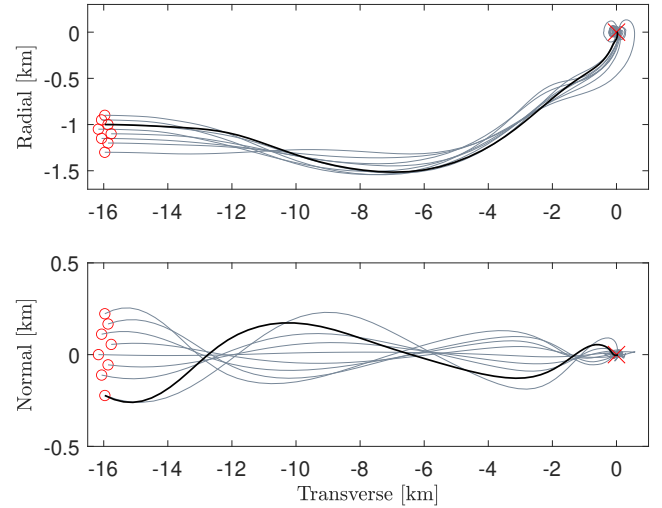


Fig. 5. Radial-vs-Transverse (top) and Normal-vs-Transverse (bottom) relative position profiles, in the presence of measurement noise and parametric uncertainty (trajectories in light gray, obtained for different initial conditions), and under nominal conditions (trajectory in black, corresponding to the results in Figs. 1-2).

to measurement noise and parametric uncertainty has been carried out. To this aim, the absolute position and velocity of the spacecraft, as well as its position and velocity relative to the rendezvous point, have been corrupted by additive white noise. The noise standard deviation is set as in Table I, according to the characteristics of standard GPS and differential GPS (DGPS) measurements. The error states (38) have then been computed from the corrupted position and velocity states. Moreover, an imperfect mounting of the thruster has been considered, by enforcing a 3 deg deviation (half-cone) between the actual thrust vector and the commanded one (this is in line with worst-case uncertainties affecting the actuation mechanism). The controller has been tested for different initial conditions close to that employed in the previous simulations, thus accounting for an off-nominal displacement between the spacecraft and the rendezvous point at the beginning of the maneuver. Figure 5 depicts the trajectories obtained in this setting. It can be seen that the spacecraft reaches the rendezvous point in all realizations. This indicates a certain degree of robustness of the design.

Finally, the vector norm-based MPC design (3) has been compared to the standard linear periodic MPC design with a quadratic cost [31], in order to highlight the main differences between these approaches. Figure 6 depicts the evolution of the state vector 2-norm obtained with the two controllers under nominal conditions. Also in this simulation, the trajectory obtained with the MPC design (3) converges in finite-time. On the other hand, the standard MPC design achieves only asymptotic regulation; the corresponding 2-norm of the input vector is depicted in Figure 7. Observe that control activation pattern lacks sparsity, as opposed to that in Fig. 2. The resulting fuel cost is $\sum_k \|u(k)\| = 44.2$, which corresponds to a propellant consumption of 11.1 g.

VII. CONCLUSIONS

An MPC strategy has been derived for linear time-periodic systems involving a sum-of-norms objective function and

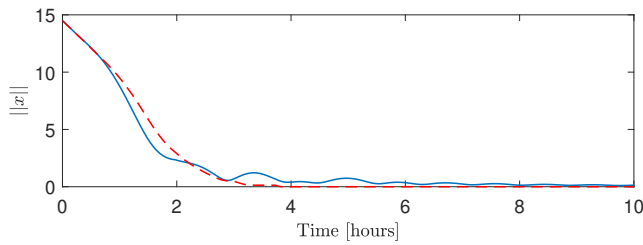


Fig. 6. 2-norm of the system state vector: MPC design (3) (red, dashed) and quadratic MPC (blue).

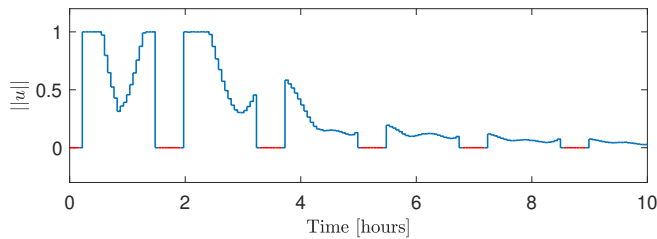


Fig. 7. Evolution of the control input vector 2-norm for the quadratic MPC (eclipse phases are highlighted in red).

norm-bound input constraints. Closed-loop exponential stability is ensured via suitable periodic terminal sets and terminal cost functions. The proposed control scheme is suitable for orbit control applications featuring intrinsically periodic phenomena such as eclipsing and orbital perturbations, and where trading off fuel consumption and tracking performance is required. Validation on a simulated realistic rendezvous problem has been carried out. Future research will focus on more complex scenarios involving, for instance, the presence of collision avoidance constraints. Furthermore, the optimization of the tuning parameters of the controller will be investigated.

REFERENCES

- [1] U. Eren, A. Prach, B. B. Koçer, S. V. Raković, E. Kayacan, and B. Açıkmeşe, “Model predictive control in aerospace systems: Current state and opportunities,” *Journal of Guidance, Control, and Dynamics*, vol. 40, no. 7, pp. 1541–1566, 2017.
- [2] S. Di Cairano, H. Park, and I. Kolmanovsky, “Model predictive control approach for guidance of spacecraft rendezvous and proximity maneuvering,” *International Journal of Robust and Nonlinear Control*, vol. 22, no. 12, pp. 1398–1427, 2012.
- [3] M. Leomanni, E. Rogers, and S. B. Gabriel, “Explicit model predictive control approach for low-thrust spacecraft proximity operations,” *Journal of Guidance, Control, and Dynamics*, vol. 37, no. 6, pp. 1780–1790, 2014.
- [4] A. Weiss, M. Baldwin, R. S. Erwin, and I. Kolmanovsky, “Model predictive control for spacecraft rendezvous and docking: Strategies for handling constraints and case studies,” *IEEE Transactions on Control Systems Technology*, vol. 23, no. 4, pp. 1638–1647, 2015.
- [5] M. Mammarella, M. Lorenzen, E. Capello, H. Park, F. Dabbene, G. Guglieri, M. Romano, and F. Allgöwer, “An offline-sampling SMPC framework with application to autonomous space maneuvers,” *IEEE Transactions on Control Systems Technology*, vol. 28, pp. 388–402, 2020.
- [6] M. Leomanni, G. Bianchini, A. Garulli, A. Giannitrapani, and R. Quartullo, “Sum-of-norms model predictive control for spacecraft maneuvering,” *IEEE Control Systems Letters*, vol. 3, no. 3, pp. 649–654, 2019.
- [7] M. Pagone, M. Boggio, C. Novara, and S. Vidano, “A Pontryagin-based NMPC approach for autonomous rendez-vous proximity operations,” in *42nd IEEE Aerospace Conference*, 2021.
- [8] H. Kiendl, J. Adamy, and P. Stelzner, “Vector norms as Lyapunov functions for linear systems,” *IEEE Transactions on Automatic Control*, vol. 37, no. 6, pp. 839–842, 1992.
- [9] F. Blanchini, “Nonquadratic Lyapunov functions for robust control,” *Automatica*, vol. 31, no. 3, pp. 451–461, 1995.
- [10] M. L. Psiaki, “Magnetic torquer attitude control via asymptotic periodic linear quadratic regulation,” *Journal of Guidance, Control, and Dynamics*, vol. 24, no. 2, pp. 386–394, 2001.
- [11] M. Lovera, E. De Marchi, and S. Bittanti, “Periodic attitude control techniques for small satellites with magnetic actuators,” *IEEE Transactions on Control Systems Technology*, vol. 10, no. 1, pp. 90–95, 2002.
- [12] B. Zhou, Z. Lin, and G.-R. Duan, “Lyapunov differential equation approach to elliptical orbital rendezvous with constrained controls,” *Journal of Guidance, Control, and Dynamics*, vol. 34, no. 2, pp. 345–358, 2011.
- [13] S. Bittanti and P. Colaneri, *Periodic Systems: Filtering and Control*. Springer-Verlag London, 2009.
- [14] G. de Nicolao, “Cyclomonotonicity, Riccati equations and periodic receding horizon control,” *Automatica*, vol. 30, no. 9, pp. 1375 – 1388, 1994.
- [15] Ki Baek Kim, Jae-Won Lee, and Wook Hyun Kwon, “Intervalwise receding horizon H_∞ tracking control for discrete linear periodic systems,” *IEEE Transactions on Automatic Control*, vol. 45, no. 4, pp. 747–752, 2000.
- [16] C. Böhm, S. Yu, and F. Allgöwer, “Predictive control for constrained discrete-time periodic systems using a time-varying terminal region,” *IFAC Proceedings Volumes*, vol. 42, no. 13, pp. 537 – 542, 2009.
- [17] R. Gondhalekar and C. N. Jones, “MPC of constrained discrete-time linear periodic systems, a framework for asynchronous control: Strong feasibility, stability and optimality via periodic invariance,” *Automatica*, vol. 47, no. 2, pp. 326–333, 2011.
- [18] F. Blanchin and W. Ukovich, “Linear programming approach to the control of discrete-time periodic systems with uncertain inputs,” *Journal of Optimization Theory and Applications*, vol. 78, no. 3, pp. 523–539, 1993.
- [19] M. Leomanni, G. Bianchini, A. Garulli, and R. Quartullo, “Sum-Of-Norms MPC for linear periodic systems with application to spacecraft rendezvous,” in *59th IEEE Conference on Decision and Control (CDC)*, 2020.
- [20] D. Mayne, J. Rawlings, C. Rao, and P. Sokaert, “Constrained model predictive control: Stability and optimality,” *Automatica*, vol. 36, no. 6, pp. 789 – 814, 2000.
- [21] J. B. Rawlings, D. Q. Mayne, and M. Diehl, *Model Predictive Control: Theory, Computation, and Design*. Nob Hill Publishing Madison, WI, 2017, vol. 2, pp. 115-116.
- [22] M. Leomanni, A. Garulli, A. Giannitrapani, and R. Quartullo, “Satellite relative motion modeling and estimation via nodal elements,” *Journal of Guidance, Control, and Dynamics*, vol. 43, no. 10, pp. 1904–1914, 2020.
- [23] R. H. Battin, *An Introduction to the Mathematics and Methods of Astrodynamics*. American Institute of Aeronautics and Astronautics, Inc., Reston, Virginia, 1999.
- [24] J. Aziz, D. Scheeres, J. Parker, and J. Englander, “A smoothed eclipse model for solar electric propulsion trajectory optimization,” *Transactions of the Japan Society for Aeronautical and Space Sciences, Aerospace Technology Japan*, vol. 17, no. 2, pp. 181–188, 2019.
- [25] W. Fehse, *Automated Rendezvous and Docking of Spacecraft*. Cambridge University Press, 2003.
- [26] M. Leomanni, A. Garulli, A. Giannitrapani, and F. Scoretcci, “Propulsion options for very low Earth orbit microsattellites,” *Acta Astronautica*, vol. 133, pp. 444–454, 2017.
- [27] T. Misuri, V. Stanzione, and N. Melega, “HT100 in-orbit validation: μ HETSat mission,” in *35th International Electric Propulsion Conference*, 2017.
- [28] M. Grant and S. Boyd, “CVX: Matlab software for disciplined convex programming, version 2.1,” <http://cvxr.com/cvx>, 2014.
- [29] L. Gurobi Optimization, “Gurobi optimizer reference manual,” 2020. [Online]. Available: <http://www.gurobi.com>
- [30] M. Leomanni, G. Bianchini, A. Garulli, A. Giannitrapani, and R. Quartullo, “Orbit control techniques for space debris removal missions using electric propulsion,” *Journal of Guidance, Control, and Dynamics*, vol. 43, no. 7, pp. 1259–1268, 2020.
- [31] C. Böhm, M. Lazar, and F. Allgöwer, “A relaxation of Lyapunov conditions and controller synthesis for discrete-time periodic systems,” in *49th IEEE Conference on Decision and Control (CDC)*, 2010, pp. 3277–3282.